

Entropic Analysis of Time Series through Kernel Density Estimation

Audun Myers^a, Bill Kay^a, Iliana Alvarez^{a,b}, Michael Hughes^a, Cameron Mackenzie^a, Carlos Ortiz Marrero^a, Emily Ellwein^a, Erik Lentz^a

^a*Pacific Northwest National Laboratory,*

^b*California State University,*

Abstract

This work presents a novel framework for time series analysis using entropic measures based on the kernel density estimate (KDE) of the time series' Takens' embeddings. Using this framework we introduce two distinct analytical tools: (1) a multi-scale KDE entropy metric, denoted as ΔKE , which quantifies the evolution of time series complexity across different scales by measuring certain entropy changes, and (2) a sliding baseline method that employs the Kullback-Leibler (KL) divergence to detect changes in time series dynamics through changes in KDEs. The ΔKE metric offers insights into the information content and “unfolding” properties of the time series' embedding related to dynamical systems, while the KL divergence-based approach provides a noise and outlier robust approach for identifying time series change points (injections in RF signals, e.g.). We demonstrate the versatility and effectiveness of these tools through a set of experiments encompassing diverse domains. In the space of radio frequency (RF) signal processing, we achieve accurate detection of signal injections under varying noise and interference conditions. Furthermore, we apply our methodology to electrocardiography (ECG) data, successfully identifying instances of ventricular fibrillation with high accuracy. Finally, we demonstrate the potential of our tools for dynamic state detection by accurately identifying chaotic regimes within an intermittent signal. These results show the broad applicability of our framework for extracting meaningful insights from complex time series data across various scientific disciplines.

1. Background & Introduction

1.1. Time Series Background

A (real valued) *time series* $\mathbf{x} = (x_1, x_2, \dots, x_t) \in \mathbb{R}^t$ is a real valued vector where $\{x_i\}_{i=1}^t$ typically represent data observations sampled at equal time intervals from some sensor or system. Time series data is ubiquitous across scientific domains including RF signal analysis, biomedical data, and dynamical systems ¹.

Email address: audun.myers@pnnl.gov (Audun Myers)

¹These are the use-cases highlighted in this document. Other frequent examples include meteorology, seismology, nuclear non-proliferation, and finance.

Broadly speaking, there are two principal modes of analysis done with time series data-forecasting (i.e., given a time series, predict what comes next) and qualitative (i.e., given a time series, analyze the data therein). In this document, we focus on the latter. In particular, in the field of dynamical systems there is a pervasive goal of classifying when (and to what extent) time series data drawn from a dynamical system is chaotic. In [4] it was observed that subsampling of time series from dynamical systems at different time scales resulted in a corresponding “unfolding of the attractor” in the dynamical system of study. In particular, the unfolding was stark when the dynamical system was periodic, present but subtler when the system was quasi-periodic, and itself chaotic when the system was chaotic.

We present methods for analyzing the degree to which the unfolding of the attractor phenomenon occurs. The methods herein apply generally to time series analysis, but we include concurrently a data driven example from scientific computing with an emphasis on RF analysis. Namely, data observations which are represented by a time series are often subjected to *noise* – that is, environmental factors, sensor precision, co-occurring signals, and other unmodeled dynamics that can introduce confounding factors which make signals difficult to analyze. A property that we are focused on is the *signal-to-noise ratio* (SNR). The SNR is a measure of the ratio of pure signal to background noise (the *power ratio*) in a given time series, and here will be measured on the decibel (dB) logarithmic scale. The degree to which Additive White Gaussian Noise (AWGN) is added to a pure RF signal is an analogue of the measure of chaos in the associated time series, and thus a study of the unfolding of the attractor as applied to RF applications is a tangible example of the general methods presented.

The presence of noise can make a time series difficult to analyze. For example, an RF signal with a sufficiently low SNR can be virtually indistinguishable from pure noise. In fact, given a time series it is often a challenge to distinguish a noisy time series which contains data from pure noise. To this end, we will discuss how to convert a time series to a point cloud which we use in Section 2.1 to classify signals by noise level. In this way, we provide a method for estimating the SNR of an unknown signal via a proxy computation.

Given a time series \mathbf{x} , we use a tool from dynamical systems analysis called *Takens’ embeddings* (via Equation 3) to turn time series into point clouds so that they can be analyzed holistically and at multiple scales using the time delay parameter τ . We remark that the structure, or lack thereof, in a Takens’ embedding of time series \mathbf{x} can change depending on (among other things) the choice of τ and the amount of structure in \mathbf{x} itself. A partially related method often used for studying time series data is through cyclostationary signal processing where the focus is on analyzing statistic properties that change periodically. Often these tools also use the delay parameter such as the autocorrelation method [9]. However, they often are not designed for and do not capture the non-linear and non-periodic behavior as is found with Takens’ embedding approaches. In Section 2.1 we will discuss in detail how to more rigorously tie the structure of a time series to its Takens’ Embedding.

1.2. Kernel Density Estimates & Entropy

Kernel Density Estimation (KDE) [1] is a method of approximating an underlying probability density function from a given data distribution. Intuitively, KDE provides a reversal

of the process of sampling (in which a probability distribution is given and data points are drawn according to that distribution); with KDE the given object is the sample and KDE gives an approximate distribution from which the data are likely to have been drawn. In Appendix B, we provide details into how KDE works and into what parameters one can select. In this document, we use a Gaussian kernel and unless otherwise noted the default parameters from the `gaussian_kde` method in the `scipy.stats` package [19].

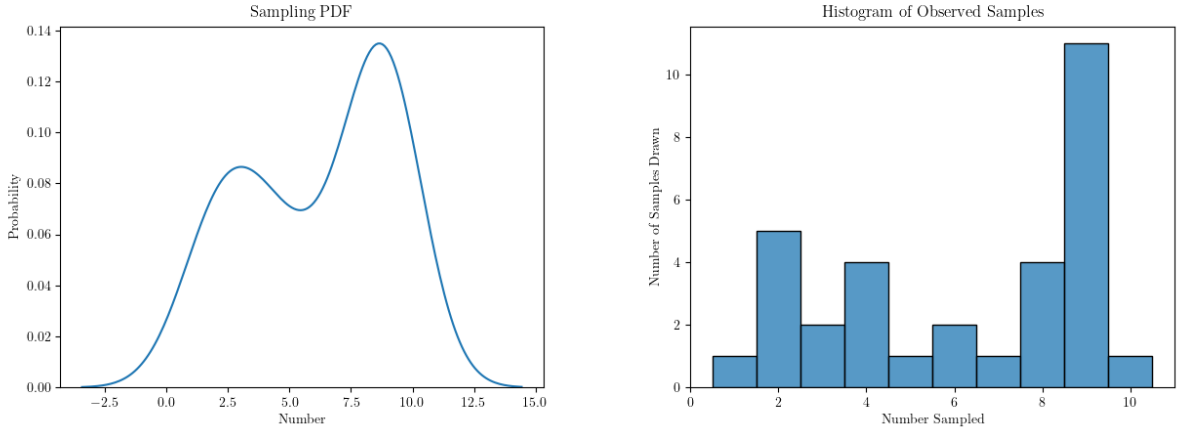


Figure 1: (Left): A probability density function used to draw integers between 0 and 10. (Right): A histogram of observed samples from an experiment sampling numbers using the PDF on the left. An experiment uses (left) to construct (right), while a KDE uses (right) to estimate (left).

While the correspondence between KDE and a histogram is readily visualized in one dimensional data (such as the number of samples drawn from a set of integers), a KDE can be computed from a point cloud in higher dimensional space. Our focus will be on KDEs of 2-dimensional Takens’ embeddings of time series, which are readily visualized as heat maps representing the heights of a two dimensional PDF.

KDEs give us a valuable tool for estimating the continuous PDF of a sampling distribution of a point cloud. Given any (discrete) random variable X with support \mathcal{X} and PDF $p(\cdot)$, the Shannon entropy of X is given by:

$$H(X) := - \sum_{x \in \mathcal{X}} p(x) \log_2 p(x) \tag{1}$$

and expresses the expected number of bits one needs to convey the outcome of X . In particular, the Shannon entropy of X is high if X is close to uniform and low if X has a varied PDF. We remark here that since a KDE provides a PDF, we can compute the entropy of a KDE. We call this measure the *KDE Entropy* (KDEE).

Closely related to the Shannon entropy of a PDF is the *Kullback-Leibler* (KL) divergence [8] between two PDFs p and q with joint support \mathcal{X} , which is defined as:

$$D(p||q) := \sum_{x \in \mathcal{X}} p(x) \log_2 \left(\frac{p(x)}{q(x)} \right), \tag{2}$$

The KL divergence is a measure of how different two PDFs are. While not a metric (failing symmetry and the triangle inequality), the KL divergence is an industry standard proxy for the distance between two distributions ². We remark that there are versions of Equations 1 and 2 for continuous random variables [2], and while many of the applications herein we are indeed working with continuous PDFs, the entropy calculations are all performed by restricting to a discrete collection of sample points and so our computational workflow handles only discretizations of continuous distributions, and so discourse on discrete entropy is most applicable to our analysis.

1.3. Summary

In this document, we propose a novel analytical workflow for analyzing time series data using entropy. Given a time series, we use tools from *topological data analysis* to produce a related point cloud. We use kernel density estimates to associate a probability distribution with the point cloud. Finally, we use entropy methods from information theory to extract valuable features from the point cloud regarding the information present in the distribution of points. We further tie the conclusions of the entropy calculations to make inference into the structure of the initial time series. In this way, we use methods from a variety of contexts to tie time series to information theory in a novel way, providing example application use-cases from RF signal processing, cardiology, and dynamical systems.

In Section 1.1, we give a primer on time series data and a method for converting time series to a point cloud. In Section 1.2, we discuss how to derive an entropy measure from general point clouds, and in Section 2.1 we relate what the KDEE of a point cloud derived from a time series signal says about the probability of detecting that signal.

In Section 3 we will demonstrate preliminary results on KDEE across various scientific domains. Section 3.1 will include a detailed explanation of the application of methods herein to *radio frequency* (RF) analysis in the presence of noise. We further include analysis of noise thresholds at which our methods are effective. Sections 3.2 and 3.3 will present preliminary results in the regimes of biomedical research (ECG) as well as dynamic systems to demonstrate the broad applicability of the methods herein.

2. Methods

In this section we outline a novel approach for analyzing time series data by way of entropic measures on the KDE of the Takens' embedding at multiple time scales (e.g., across multiple choices of τ). We first introduce a measure of how much signal information there is in a single time series by measuring the change in entropy associated to the unfolding of the signal as the time scale increases. The second approach is based on measuring of the difference between the maximum entropic changes of a section of a signal in comparison to a previous section of signal for change point and detecting signal injections. We begin by first providing a complete example of our methodology for computing the KDE from a

²One reason for this is that the KL divergence is the expected log-likelihood ratio between two distributions [8]. For an overview of KL divergence, see [2].

signal in Section 2.1 and then provide details on our two entropic measures using the KDE in Sections 2.2 and 2.3.

2.1. Time Series and KDE

To illustrate our methodology we will use a simple sinusoidal signal example that can be related to each step. This example is demonstrated in Fig. 2.

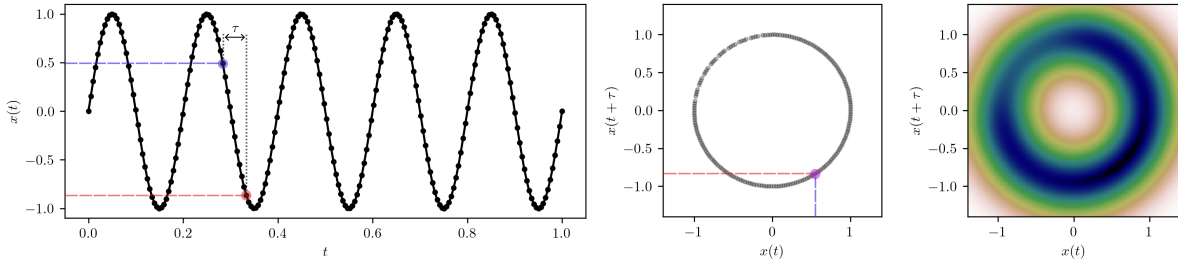


Figure 2: A sinusoidal wave, its Takens' embedding, and a KDE of the Takens' embedding.

Our method begins with a time series $\mathbf{x} = (x_1, x_2, \dots, x_t) \in \mathbb{R}^t$ (see left subfigure of Fig 2). We next perform a Takens' embedding in two dimensions by selecting a time delay and delay upper bound $\tau, N \in \mathbb{N}$ then computing the two-dimensional Takens' embeddings as

$$P_\tau(\mathbf{x}) := \{(x_i, x_{i+\tau})\}_{i=1}^{t-N} \text{ for } 1 \leq \tau \leq N. \quad (3)$$

An example point $p \in P_\tau(x)$ is shown in both the signal on the left subfigure with the τ time delay spacing and the Takens' embedding point cloud in the middle subfigure of Fig. 2. Using the point cloud $P_\tau(\mathbf{x})$, we take a Kernel Density Estimate (KDE) using a Gaussian kernel³. Denote this estimate $K(P_\tau(\mathbf{x}))$. The example KDE is shown on the right of Fig. 2.

2.2. Kernel Density Estimate Entropy (KDEE)

Deriving the KDE from a signal we can compute the Shannon entropy $H(K(P_\tau(\mathbf{x})))$ produce the entropy of the KDE, which we refer to as the (τ) -KDEE of \mathbf{x} , denoted as

$$\text{KE}_\tau(\mathbf{x}) := H(K(P_\tau(\mathbf{x}))). \quad (4)$$

While $\text{KE}_\tau(\mathbf{x})$ is a real value and has applications in measuring the complexity of a signal, we have found that it is fairly dependent on qualitative properties of \mathbf{x} , and for fixed τ is limited in its usefulness. This is because τ as a time delay parameter for the Takens' embedding is agnostic to certain qualitative properties of \mathbf{x} . For example, if \mathbf{x} and \mathbf{x}' are observations of the same phenomenon but \mathbf{x}' is sampled twice as frequently as \mathbf{x} , then $\text{KE}_\tau(\mathbf{x}) = \text{KE}_{2\tau}(\mathbf{x}')$ for even indices of \mathbf{x}' . Thus, factors such as sampling frequency can have an impact on

³Experiments herein were performed using the `gaussian_kernel` from the `scipy.stats` [19] package with default parameters.

$KE_\tau(\cdot)$ and are also independent of τ . To this end, we consider the evolution of $KE_\tau(\cdot)$ at multiple time-scales with respect to τ . That is, we analyze the evolution of $KE_\tau(\cdot)$ over a range of choices for τ rather than for a fixed choice of τ . In the instance of an RF signal, the change in $KE_\tau(\cdot)$ is correlated to the SNR, and in general dynamical systems with a greater change in $KE_\tau(\cdot)$ seem to be correlated to the degree to which the attractor of the system unfolds. To this end, we propose the following parameter for capturing the total variance of KDEE for a time series \mathbf{x} as

$$\Delta KE(\mathbf{x}) = \left| \max_{\tau} KE_\tau(\mathbf{x}) - \min_{\tau^*} KE_{\tau^*}(\mathbf{x}) \right|. \quad (5)$$

We demonstrate this for our previous simple sinusoidal time series but now for multiple τ shown in Fig. 3a.

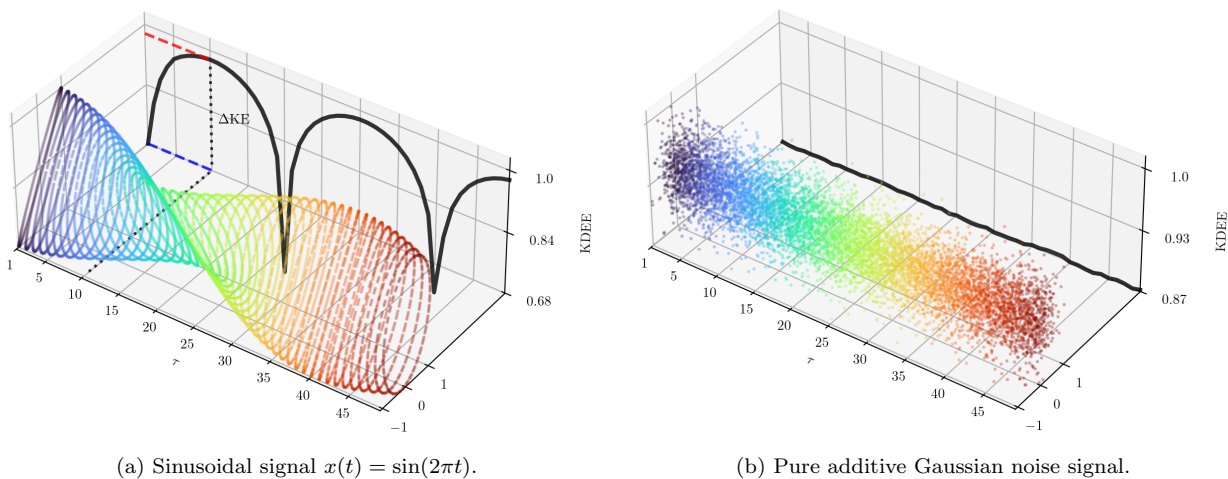


Figure 3: Example unfolding of point cloud embedding as τ increases with corresponding change in KDEE (KE_τ) on the example signal in Fig. 2 as well as pure Gaussian noise.

One observation is that ΔKE serves as a proxy for SNR. Heuristically, we observed that signals with low SNR have a small ΔKE while signals with a high SNR have a relatively large ΔKE . For example, in Fig. 3b shows the multi-scale KDEE for pure Gaussian noise which shows no unfolding of the point cloud embedding and as such has a very low ΔKE compared to that of the sinusoidal signal. We show this relation between signal and noise amplitude heuristically in more detail in Appendix A.

In practice, computing $KE_\tau(\mathbf{x})$ is relatively fast for a fixed τ , and so $\Delta KE(\mathbf{x})$ can be approximated by searching over a sufficiently large range of choices of τ and taking the smallest value (frequently, $\tau = \epsilon$) and the largest value.

2.3. Sliding Baseline Change Detection

To detect changes in signal dynamics we can also use the KDEE by measuring the entropic change in its distribution over time. To do this we use a sliding baseline method compared to a window of interest in a given signal. To illustrate this process we have outlined an artificial

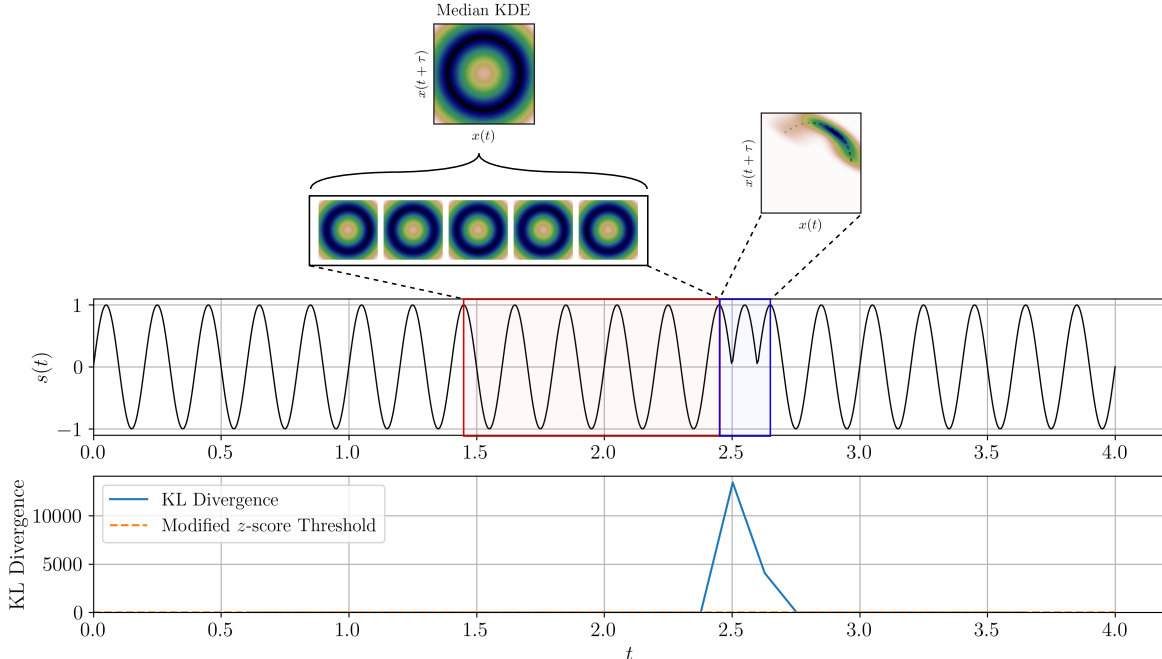


Figure 4: Example demonstrating change detection using KL divergence of the median KDE of a baseline (red window) and a window of interest (blue window).

example in Fig. 4. Here we have a signal that is a simple sinusoid wave $x(t) = \sin(2\pi t)$ except during a brief period around time $t = 2.5$ where the signal is modified to $\bar{x}(t) = |\sin(2\pi t)|$.

Our method is based on a sliding baseline procedure where we take the previous W windows (highlighted in red and in this case $W = 5$) and calculate the KDE for each. We then take the point-wise median of the KDE as our baseline. We use the median as it is robust to outliers making the method capable of having previous injection data within the baseline. So long as the baseline consists of at least 50% true baseline data (e.g., benign data in an anomaly detection setting), we can use the median baseline.

We next compare the median KDE to the window of interest (highlighted in blue) and measure the difference between them. The *KL* divergence (Equation 2) is a measure of the difference between probability distributions, it suffers from a lack of symmetry; the divergence from distribution P to Q differs from Q to P . To address this, symmetrized versions have been developed. A straightforward approach involves taking the average of the *KL* divergences in both directions, effectively quantifying the total dissimilarity regardless of direction. This simple average of

$$\bar{D}_{KL}(P, Q) = \frac{1}{2}(D_{KL}(P||Q) + D_{KL}(Q||P)) \quad (6)$$

yields a direct symmetric measure of dissimilarity. Alternatively, the Jensen-Shannon divergence [10] could be used as it offers a more nuanced approach by measuring the average

divergence to the midpoint distribution. Additionally, to deal with the problem of zeros in the prior distribution (i.e., to avoid infinite values in our KL-divergence calculation), we add a regularization constraint to both distributions of $0.001 \max(P)$ and $0.001 \max(Q)$ to both P and Q , respectively, before calculating the KL divergence.

To detect a significant change in the signal from the baseline we use the modified z -score which is calculated as

$$Z = \frac{0.6745(X - \text{median}(X))}{\text{MAD}}. \quad (7)$$

When seeking to identify outliers or significant deviations within a dataset, the modified z -score offers a robust alternative to the traditional z -score. Unlike its standard counterpart, which relies on the mean and standard deviation, the modified z -score centers on the median and the median absolute deviation (MAD). This choice makes it less susceptible to the influence of extreme values, which can skew the mean and standard deviation. Essentially, it quantifies how far a data point lies from the median, expressed in units that approximate standard deviation. In our work we consider a value an outlier if the modified z -score is greater than 3.5 which is shown in Fig. 4 near 0 on the bottom figure as there is little deviation from the median.

The example in Fig. 4 Demonstrates how KDE and KL divergence can be combined to detect changes in a signal by detecting an entropic based change in the signal’s structure.

3. Results

In this section, we implement our KDE-based entropic signal measures to time series in various domain sciences. Namely, in Section 3.1, we give a detailed breakdown of the methods herein applied to a set of realistic simulated RF signals across multiple signal-to-noise and signal-to-interference ratios with a comparison to state-of-the-art methods such as an autoencoder with details on the implementation provided in Appendix D. In Section 3.2, we give select results from ECG data and the detection of ventricular fibrillation. In Section 3.3, we show how this method has potential for dynamic state detection in a dynamical system exhibiting intermittency with a changing dynamic state from periodic to chaotic.

3.1. Radio Frequency Signal Processing for Injection Detection

Radio frequency (RF) signals, occupying the spectrum from 30 kHz to 300 GHz [16], are frequently recorded as time series, denoted as \mathbf{x} . These time series capture the oscillatory nature of signals propagating through diverse media. While the transmission of RF signals often involves modulation and demodulation processes, this work centers on the detection of informative signals within noisy environments, irrespective of the particular modulation scheme employed and before the signals are demodulated (over-the-air signals [12]). This approach broadens the applicability of our methods to encompass a range of modulation techniques, a consideration of practical significance in RF signal analysis. Although modulation/demodulation is not explicitly modeled here, and while entropy-based methods have been explored for classifying received signals based on modulation type [7], we concentrate on the core problem of signal identification in the presence of noise and signal interference.

The primary goal of this investigation is to detect the injection of signals into a noisy environment. We employ simulated signals generated following the general framework presented in [12], which provides control over the Signal-to-Noise Ratio (SNR)⁴. However, we additionally provide realistic background interference by simulating a narrow frequency band of background signals as would be seen in a congested frequency domain. We provide details on the background interference simulation in Appendix C.1.

A data-driven heuristic analysis, detailed in Appendix A, suggests that changes in entropic value of the KDE of the Takens’ embedding are indicative of the SNR of an unknown signal. Building upon this observation, we demonstrate our novel injection and change-point detection algorithm based on entropic measure of the KDE to identify both the presence and the temporal location of injected signals. Additionally, we use our sliding baseline entropic comparison of the KDEs approach outlined in Section 2.3. The performance of these detectors is benchmarked against standard signal processing approaches (e.g., Fourier spectrum analysis) and state-of-the-art change point detection methodologies (e.g., autoencoder (AE)-based anomaly detection). In our comparison methods we did not use energy based approaches as for many of the applications there is no change in the energy of the signal as the state changes.

Test Data Generation. For our experiments, we leveraged and adapted the signal generation tool described in [12] to create a dataset of injected RF signals into a noisy domain with background interference signals. Ten signals were generated for each of the 14 supported modulation types over all background simulations. Each signal comprised 5000 samples and 100 symbols (50 samples per symbol), representing a 1-second interval at an root-mean-squared amplitude of 1. A raised-cosine filter with a roll-off factor of 0.25 ($RRC_\alpha = 0.25$) was employed. Both additive Gaussian noise and interference background signals were introduced to achieve the target Signal-to-Noise Ratio (SNR) and Signal-to-Interference Ratio (SIR). A description of the interference signal is provided in Appendix C.1. In this work we are calculating the SNR as using the ratio of signal and noise power estimated from the root-mean-square value of each, which is described in detail in Appendix C.2.

A randomly selected time window within the latter half of each signal was designated as the injection interval. The duration of the injected pulse was randomly selected between 20% and 40% of the signal length. During the injection period, the signal of the specified SNR, SIR, and modulation type was superimposed onto the noise. Outside this period, only noise and background signal was present.

In Fig. 5 we demonstrate our procedure on a sample signal with generated signal with an $SIR = SNR = 4$ and BPSK modulation. In this figure the 10 baseline KDEs and the corresponding window of time (highlighted in red) are shown with their median. Additionally, the window of interest (highlighted in blue) and its corresponding KDE are shown where there is a transition from background signal to the true injection. On the bottom subfigure demonstrate both the KL divergence and the ΔKE methods for detecting this injection with

⁴This simulator includes 14 modulation formats: BPSK, QPSK, OQPSK, Pi4QPSK, 8PSK, 16PSK, OOK, 4ASK, 8ASK, 16QAM, 64QAM, 32QAM, 16APSK, and 32APSK.

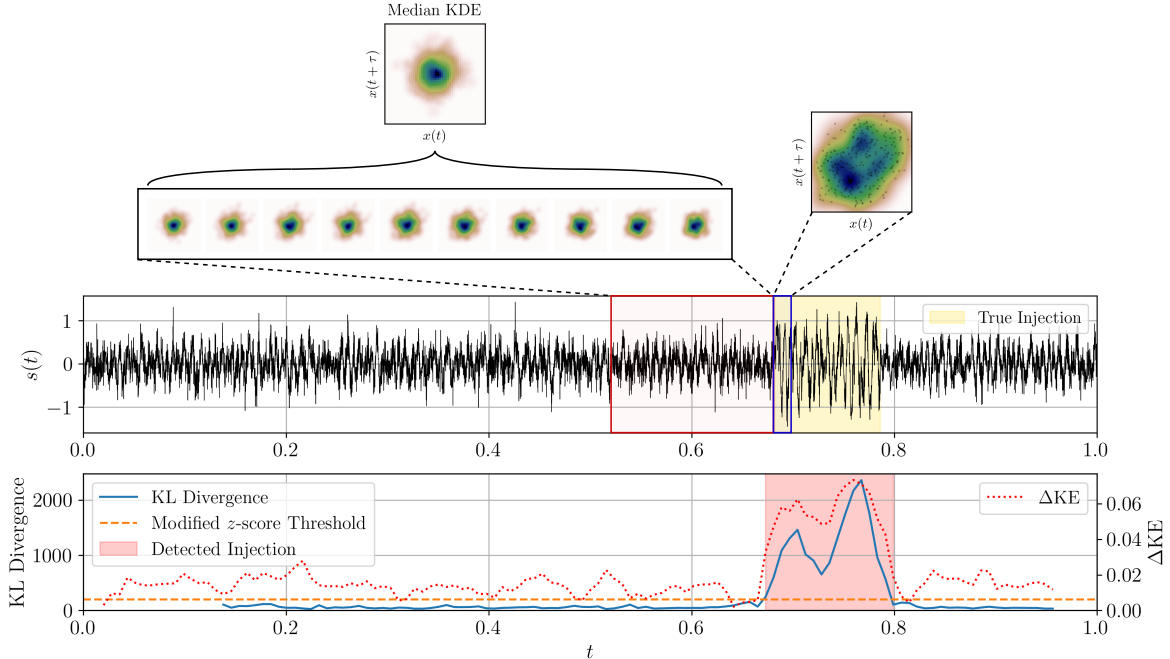


Figure 5: Example RF Signal injection with background interference and noise as well as sliding baseline (10 KDEs) and window of analysis.

the modified z -score threshold shown for the KL divergence. Both approaches show a clear increase during the injection for this example with the red region in the lower subfigure highlighting the detected injection based on the KL divergence.

Noise robustness Analysis. In this section, we conduct a comparative analysis of radio frequency (RF) signal injection detection performance. We evaluate two distinct anomaly detection methodologies: Kullback-Leibler divergence (KL) and Autoencoder (AE) based approaches. Additionally we compare these to our ΔKE approach as we are attempting to detect signal in a noisy environment. Our evaluation spans a range of Signal-to-Noise Ratio (SNR) and Signal-to-Interference Ratio (SIR) values, allowing us to assess performance under varying signal conditions. To ensure a comprehensive assessment of robustness, we employ three distinct data representations: raw time series (TS) data, power spectral density (PSD) representations, and kernel density estimates (KDE) derived from the Takens' embedding, thereby capturing diverse signal characteristics.

To quantify and compare the detection performance of these methods, we employ the F_1 score. The F_1 score, a harmonic mean of precision and recall, provides a balanced measure of detection accuracy, specifically calculated between the true and detected injection intervals along the time axis. For calculating the F_1 score we detect if at least 25% of the given window is overlapping with the known ground truth injection. If it is then we flag the window as an injection.

We present the F_1 scores with standard deviation error bars, derived from ten indepen-

dent trials at each combination of modulation type and background signal, to illustrate the variability and reliability of our results. These result are shown in Fig. 6. We note that minimal performance variation was observed across different modulation types, suggesting that both KL and AE-based approaches exhibit a degree of modulation independence.

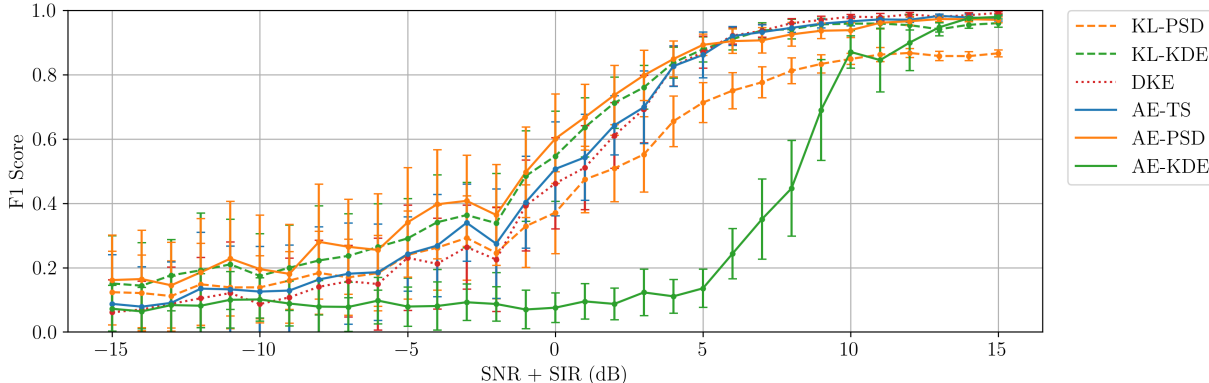


Figure 6: RF signal injection detection performance comparison of Kullback-Leibler divergence (KL) and Autoencoder (AE) based anomaly detection across varying Signal-to-Noise Ratio (SNR) and Signal-to-Interference Ratio (SIR). Methods evaluated using raw Time Series (TS), Power Spectral Density (PSD), and Kernel Density Estimate (KDE) of Takens’ embedding.

Each data representation is paired with a detection method as representation-method (e.g., KL-KDE is KL divergence of the Kernel Density Estimate). We remark here that of top three performant methods (KL-KDE, AE-TS, and AE-PSD), the KL-KDE method is the only one that does not require the training and deployment of an Autoencoder, and in fact is orders of magnitude faster to deploy while achieving comparable performance to the standard methods with ML components. This suggests that KDEE is a suitable tool for application spaces where data is streaming and requires real time change detection. We also found that the ΔKE (DKE) method⁵ did not perform as well as the KL-KDE approach; however, it does not require a baseline comparison giving it a significant advantage in spaces where there is insufficient data to create a baseline.

By examining the computational demands of each detection method, as presented in Table 1, we observe notable differences in processing time. KL Divergence-based methods demonstrate a clear advantage in computational efficiency compared to Autoencoder-based techniques. This disparity arises from the inherent complexity of Autoencoder training and inference, which involves substantial matrix operations and iterative optimization, whereas KL Divergence calculations are comparatively less demanding. Although the ΔKE method exhibits processing speeds similar to Autoencoders, its detection performance falls short of the KL Divergence approach applied to Kernel Density Estimates (KDE). These findings highlight the computational benefits of KL Divergence-based methods, especially when rapid

⁵The computation time includes finding the τ corresponding to a maxima in KE_τ .

Table 1: Mean compute time for a single RF signal with sliding windows.

Detection Method	Vectorization Method	Mean Compute Time (Seconds)
Autoencoder	Time Series	0.441
	Power Spectral Density	0.387
	Kernel Density Estimate	0.523
KL Divergence	Power Spectral Density	0.018
	Kernel Density Estimate	0.066
Δ KE		0.398

signal analysis and real-time detection capabilities are paramount.

3.2. ECG Data Analysis

Electrocardiography (ECG) data are time-series representations of cardiac signals that are often used to diagnose various medical conditions [6] [20]. In particular, anomalies in an ECG reading can correspond to cardiac events of interest to diagnosticians. Various methods (both Machine Learning and qualitative domain knowledge) are applied to ECG time series towards anomaly detection for improving diagnostic tools ⁶ for cardiac incidents. To this end, ECG data provides us with well curated time series data for anomaly detection tasks to be benchmarked on. Here, we show the performance of our entropic KDE statistics on the CU Ventricular Tachyarrhythmia Database [11] [5]. ⁷ From the physionet database, 35 eight-minute ECG recordings were analyzed of human subjects who experienced episodes of sustained ventricular tachycardia, ventricular flutter, and ventricular fibrillation. Each ECG signal is labeled with the state of the patient. In this work any Ventricular Fibrillation (VF) related state is labeled as VF and our goal is to detect regions of VF as a binary application (i.e., normal compared to abnormal using state change detection).

An example of our methodology applied to an ECG signal from the ECG dataset is shown in Fig. 7. Highlighted in red on the signal subfigure is an example baseline and in blue is the window of interest. For each window we calculate the KL divergence of the windows KDE compared to the median of the baseline. The resulting KL divergence values are shown in the bottom subfigure with the red region indicating the detected ventricular fibrillation where the KL divergence was greater than the modified z -score threshold. As shown, the detect region aligns with the ventricular fibrillation with largely overlapping intervals in this example.

Over the entire ECG dataset we calculated the F_1 score. We report our results in Table 2. This table shows that the KL divergence paired with the KDE of the Takens' embedding achieved the highest F_1 score compared to all of the tested methods.

⁶We remark that we are making no claims about the clinical efficacy of our methods herein – development of entropic measures of KDE for diagnostic purposes would require future collaboration with appropriate clinicians.

⁷The database used can be found at: physionet.org.

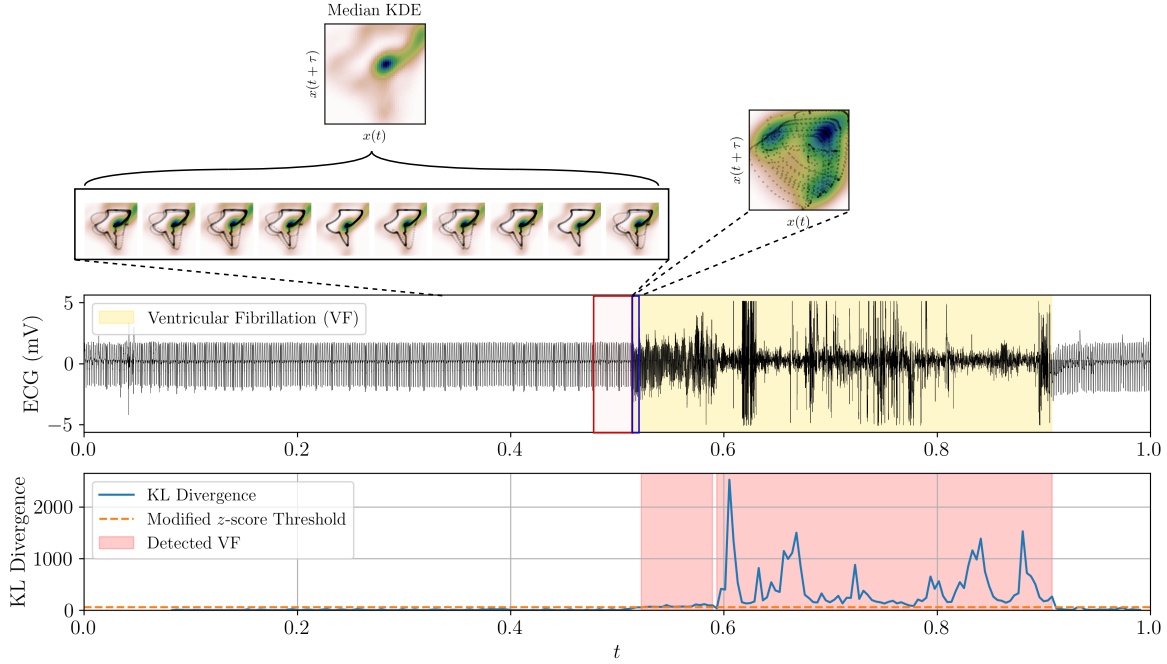


Figure 7: Example ECG signal with sliding baseline with median KDE compared to window of interest. Resulting detected VF window (red) compared to true VF window (yellow).

Table 2: Ventricular fibrillation detection results.

Detection Method	Vectorization Method	F1 Score
Autoencoder	Time Series	80.3% \pm 12.1%
	Power Spectral Density	81.2% \pm 13.1%
	Kernel Density Estimate	62.5% \pm 16.3%
KL Divergence	Power Spectral Density	77.8% \pm 10.2%
	Kernel Density Estimate	87.1% \pm 8.7%

3.3. Dynamic State Detection

In this section we demonstrate how our entropy statistics on the KDE can be used for identifying periodic and chaotic regimes within intermittent signal (characterized by irregular transitions between periodic and chaotic behavior) [15]. The analysis focuses on the x variable of the Lorenz system defined as

$$\begin{aligned}
 \frac{dx}{dt} &= \sigma(y - x), \\
 \frac{dy}{dt} &= x(\rho - z) - y, \\
 \frac{dz}{dt} &= xy - \beta z.
 \end{aligned}
 \tag{8}$$

which was simulated using the `teaspoon` [9] python package and using the standard parameters $\sigma = 10$, $\beta = 8/3$, and $\rho = 166.18$, which exhibit type-I intermittency [15]. The system was numerically integrated at 150 Hz for 1000 seconds, with the initial 93 seconds discarded to ensure the system’s dynamics were fully developed.

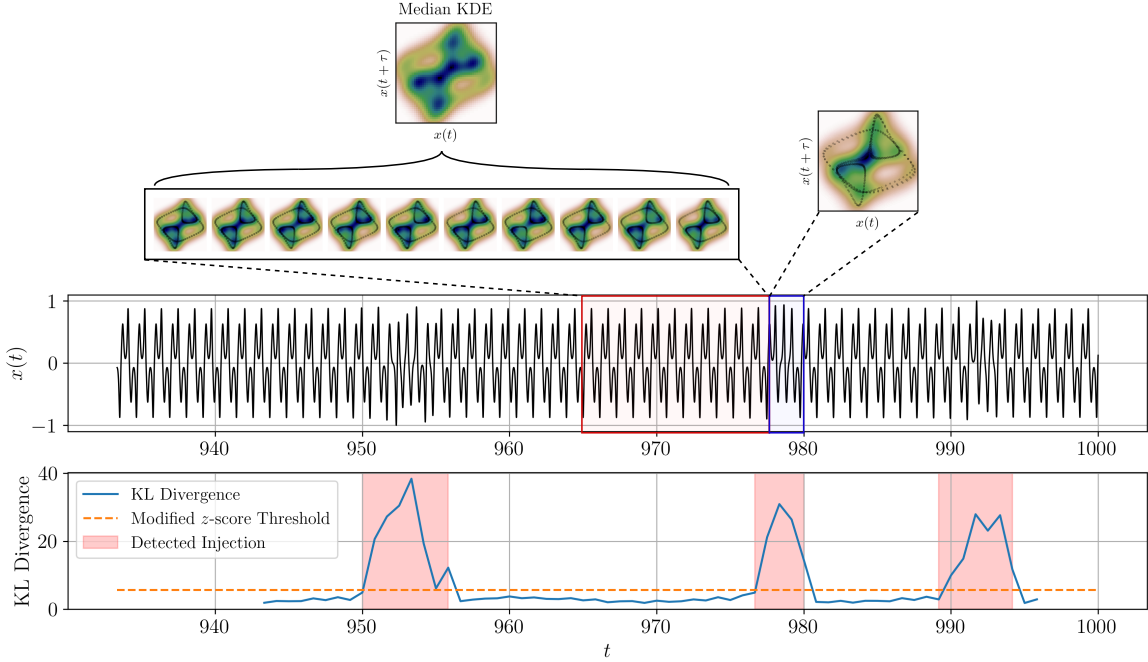


Figure 8: Example signal demonstrating intermittency in the Lorenz dynamical system 8 for the detection of chaotic intervals with sliding baseline (10 KDEs) and window of analysis.

Figure 8 illustrates the time series of $x(t)$ and the resulting detecting chaotic intervals. As shown in the bottom subfigure, there are peaks in the KL divergence during chaotic regions of the signal. This results shows the diverse applicability and generality of our entropic KDE approaches to detecting changes in signals and opens the avenue for future research in KDE applied to studying dynamical systems.

4. Conclusion

In this document, we introduced a novel analytical pipeline for analyzing qualitative properties of time series by transforming them into point clouds, approximating the point clouds with a PDF, and computing the entropy of the resulting PDF. Each part of the pipeline is modular, and applies to general instances of their respective inputs. The novelty lies in tying the final output (KDEE) to the initial input (a time series). We demonstrated that conclusions could be drawn about time series from KDEE in three distinct data driven use-cases- RF signal processing, cardiology, and dynamical systems. These were three instances where changes in qualitative properties of time series are of interest to domain scientists;

here we are introducing the method of KDEE for time series analysis in the literature but remark that this set of use-cases is not the totality of the scope of the method. Further, the results herein are intended to be a proof-of-concept application. For future work, we encourage domain scientists whose primary data of interest are time series for which change point detection is important.

5. Acknowledgements

This work is funded by the Pacific Northwest National Laboratory. Pacific Northwest National Laboratory information release number PNNL-SA-209698.

References

- [1] Yen-Chi Chen. A tutorial on kernel density estimation and recent advances. *Biostatistics & Epidemiology*, 1(1):161–187, 2017.
- [2] Thomas M Cover and Joy A Thomas. Information theory and statistics. *Elements of information theory*, 1(1):279–335, 1991.
- [3] Richard A Davis, Keh-Shin Lii, and Dimitris N Politis. Remarks on some nonparametric estimates of a density function. *Selected Works of Murray Rosenblatt*, pages 95–100, 2011.
- [4] Andrew M Fraser and Harry L Swinney. Independent coordinates for strange attractors from mutual information. *Physical review A*, 33(2):1134, 1986.
- [5] Ary L Goldberger, Luis AN Amaral, Leon Glass, Jeffrey M Hausdorff, Plamen Ch Ivanov, Roger G Mark, Joseph E Mietus, George B Moody, Chung-Kang Peng, and H Eugene Stanley. Physiobank, physiotoolkit, and physionet: components of a new research resource for complex physiologic signals. *circulation*, 101(23):e215–e220, 2000.
- [6] Shenda Hong, Cao Xiao, Tengfei Ma, Hongyan Li, and Jimeng Sun. Mina: multilevel knowledge-guided attention for modeling electrocardiography signals. *arXiv preprint arXiv:1905.11333*, 2019.
- [7] Bill Kay, Audun Myers, Thad Boydston, Emily Ellwein, Cameron Mackenzie, Iliana Alvarez, and Erik Lentz. Permutation entropy for signal analysis, 2024.
- [8] Solomon Kullback and Richard A Leibler. On information and sufficiency. *The annals of mathematical statistics*, 22(1):79–86, 1951.
- [9] Audun D Myers, Melih Yesilli, Sarah Tymochko, Firas Khasawneh, and Elizabeth Munch. Teaspoon: A comprehensive python package for topological signal processing. In *TDA {\&} Beyond*, 2020.

- [10] Frank Nielsen. On the jensen–shannon symmetrization of distances relying on abstract means. *Entropy*, 21(5):485, 2019.
- [11] FM Nolle, FK Badura, JM Catlett, RW Bowser, and MH Sketch. Crei-gard, a new concept in computerized arrhythmia monitoring systems. *Computers in Cardiology*, 13(1):515–518, 1986.
- [12] Timothy James O’Shea, Tamoghna Roy, and T Charles Clancy. Over-the-air deep learning based radio signal classification. *IEEE Journal of Selected Topics in Signal Processing*, 12(1):168–179, 2018.
- [13] Byeong U Park and James S Marron. Comparison of data-driven bandwidth selectors. *Journal of the American Statistical Association*, 85(409):66–72, 1990.
- [14] Emanuel Parzen. On estimation of a probability density function and mode. *The annals of mathematical statistics*, 33(3):1065–1076, 1962.
- [15] Yves Pomeau and Paul Manneville. Intermittent transition to turbulence in dissipative dynamical systems. *Communications in Mathematical Physics*, 74:189–197, 1980.
- [16] Jessica Scarpati. What is radio frequency (rf, rf)? *SearchNetworking.*, URL: <https://www.techtarget.com/searchnetworking/definition/radio-frequency> (18.9.2022.), 2021.
- [17] David W Scott. *Multivariate density estimation: theory, practice, and visualization*. John Wiley & Sons, 2015.
- [18] Bernard W Silverman. *Density estimation for statistics and data analysis*. Routledge, 2018.
- [19] Pauli Virtanen, Ralf Gommers, Travis E. Oliphant, Matt Haberland, Tyler Reddy, David Cournapeau, Evgeni Burovski, Pearu Peterson, Warren Weckesser, Jonathan Bright, Stéfan J. van der Walt, Matthew Brett, Joshua Wilson, K. Jarrod Millman, Nikolay Mayorov, Andrew R. J. Nelson, Eric Jones, Robert Kern, Eric Larson, C J Carey, İlhan Polat, Yu Feng, Eric W. Moore, Jake VanderPlas, Denis Laxalde, Josef Perktold, Robert Cimrman, Ian Henriksen, E. A. Quintero, Charles R. Harris, Anne M. Archibald, Antônio H. Ribeiro, Fabian Pedregosa, Paul van Mulbregt, and SciPy 1.0 Contributors. SciPy 1.0: Fundamental Algorithms for Scientific Computing in Python. *Nature Methods*, 17:261–272, 2020.
- [20] Yadong Zhang and Xin Chen. Anomaly detection in time series with triadic motif fields and application in atrial fibrillation ecg classification. *arXiv preprint arXiv:2012.04936*, 2020.

Appendix A. Correlation Between ΔKE and SNR

In this appendix, we present a heuristic correlation between SNR and ΔKE to motivate ΔKE as a feature of interest in RF signal processing. In practice, the SNR of an observed signal is not a known quantity. Here, we demonstrate that ΔKE is correlated with SNR at various sampling rates, and when the sampling rate is known or approximable, ΔKE serves as a reliable proxy for SNR in fairly noisy (approx. -10dB) regimes. The unknown SNR of a signal can be of interest to domain practitioners, and ΔKE can be observed directly from a signal. The general correlation of “change in ΔKE implies change in SNR” motivates the use of ΔKE as a changepoint detector, and the heuristic accuracy bars motivate using ΔKE as a proxy when sampling rate is known. To this end, we ran an experiment where, using the signal simulation methods of [12], we generated a corpus of 10 signals of each available modulation type at SNRs between -10 and 11 at 3 dB steps and computed the ΔKE values for each. The generated signals were length 3000 and then downsampling the signals by a rate of 2, 3, and 4 bits. In Figure A.9, we plot the mean and standard deviation of the results for each SNR averaged across modulation types.

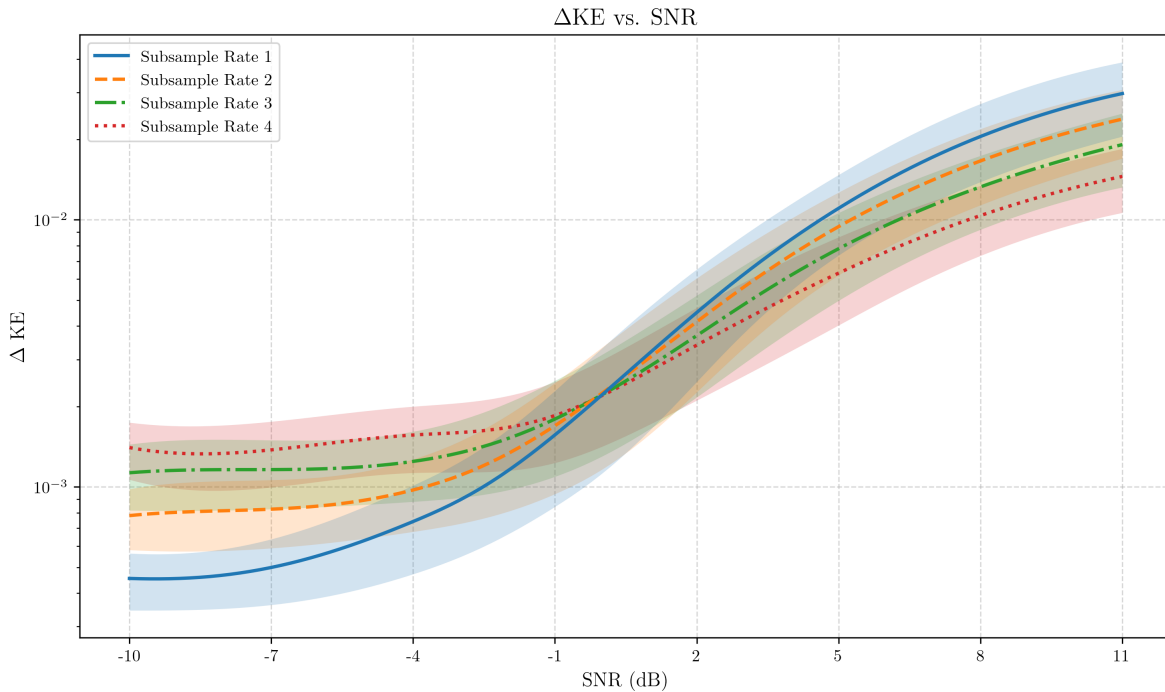


Figure A.9: For each SNR, 10 signals of each of 14 modulation types were generated. The ΔKE of each signal was computed. Plotted are the means with one standard deviation across all modulation types on a log scale to show correlation between SNR and ΔKE .

Further, there is not much variation in the correlation between ΔKE and SNR for individual modulation types, suggesting that this feature is a useful correlation (and with

additional knowledge, a useful proxy) in the context where the signal modulation type is unknown.

Appendix B. Kernel Density Estimation (KDE)

In this appendix, we provide relevant background on kernel density estimation towards keeping the methods of this document self-contained. For a thorough treatment of kernel density estimates, see [1].

Developed independently by Parzen and Rozenblatt [14][3] kernel density estimation provides a partial answer to the following question:

Question 1. *Given (x_1, x_2, \dots, x_n) a set of samples from \mathbb{R}^d drawn independently and identically distributed from an unknown pdf f , how can we estimate f ?*

A partial answer to this question is provided by the (family of) *kernel density estimates* with *kernel* K and smoothing *bandwidth* parameter h (denoted $\hat{f}_{h,K}$), which are formally defined as:

$$\hat{f}_{h,K}(x) := \frac{1}{nh^d} \sum_{i=1}^n K\left(\frac{x - x_i}{h}\right)$$

where $K : \mathbb{R}^d \rightarrow \mathbb{R}$ is a smooth function called a *kernel* and $h > 0$ is called a bandwidth parameter. Selection of K and h is itself an active research area, but absent external domain knowledge steering a decision, a common choice (and the one made in this document) for K is the *gaussian kernel* $\phi(x)$, given by the pdf for the standard normal distribution:

$$\phi(x) = \frac{1}{\sqrt{2\pi}} \exp\{-x^2/2\}.$$

Selecting h is a difficult problem, with entire works dedicated to the survey of bandwidth selection (see, e.g., [13]). Choosing a bandwidth is a balance between under and over smoothing; an optimal choice of bandwidth typically seeks to minimize the *mean integrated square error*:

$$\text{MISE}(h) := \mathbb{E} \left\{ \int \left(\hat{f}_{h,K}(x) - f(x) \right)^2 dx \right\}$$

where f is the (unknown) density function. Since f is unknown, the argmin of MISE cannot be computed directly. Machine learning techniques or data driven heuristics can be applied. The two most common plug in methods are *Scott's Method* [17] and the *Silverman Method* [18] which are each built in to SciPy's `gaussian_kde` method. For our use-case, the default Scott's method was sufficient; in this application h is computed as:

$$n^{-1/(d+4)}$$

where n is the number of points sampled and d is the ambient dimension of the point set.

Appendix C. Noise and Interference Calculations

Appendix C.1. SIR

To simulate realistic background interference, we create a narrow-band signal composed of multiple sub-channels. We model this as four distinct channels, each with a bandwidth of 5 MHz, separated by 5 MHz gaps. Each of these four channels is further divided into five sub-channels (each with a 1 MHz width), resulting in a total of 20 sub-channel background signals. Each sub-channel carries a unique modulated signal, generated from a random bit sequence. The modulation type for each channel (and all its sub-channels) is randomly selected from a set of 14 possible digital modulation schemes, as detailed in Section 3.1.

The power of this simulated background interference is then adjusted to achieve a specific Signal-to-Interference Ratio (SIR). This ensures the background interference has a controlled level of power relative to the primary signal, enabling us to test the system's performance under realistic interference conditions. To modify the amplitude of the background signal we sum them as $B(t) = \sum b(t)$ where $b(t)$ is a single sub-channel signal. This summing is based on what the observations of the background would be if filtered the entire RF spectrum to this bandwidth. The amplitude of $B(t)$ is then scaled according to the injection signals amplitude as

$$A_{B(t)} = \sqrt{\frac{P_{\text{injection}}}{10^{\frac{\text{SIR}_{\text{dB}}}{10}}}} \quad (\text{C.1})$$

where $A_{B(t)}$ is the amplitude of the combined background signal $B(t)$, $P_{\text{injection}}$ is the power of the injection signal, and SIR_{dB} is the desired Signal-to-Interference Ratio in decibels.

Appendix C.2. SNR

To determine the appropriate noise amplitude for a given signal and target Signal-to-Noise Ratio (SNR), we proceed as follows:

1. **SNR Conversion:** We begin with the desired SNR expressed in decibels (SNR_{dB}) and convert it to a linear scale (SNR) using the following relationship:

$$\text{SNR} = 10^{\frac{\text{SNR}_{\text{dB}}}{10}} \quad (\text{C.2})$$

2. **Signal Power Calculation:** We then calculate the power of the signal (P_{signal}) as the mean of the squared signal values:

$$P_{\text{signal}} = \frac{1}{N} \sum_{i=1}^N s[i]^2 \quad (\text{C.3})$$

where N represents the number of samples in the signal s .

3. **Noise Power Determination:** With the linear SNR and signal power in hand, we calculate the required noise power (P_{noise}) using the definition of SNR:

$$\text{SNR} = \frac{P_{\text{signal}}}{P_{\text{noise}}} \implies P_{\text{noise}} = \frac{P_{\text{signal}}}{\text{SNR}} \quad (\text{C.4})$$

4. **Noise Amplitude (Standard Deviation):** Assuming additive white Gaussian noise (AWGN) with zero mean, the noise amplitude is represented by its standard deviation (σ). This standard deviation is related to the noise power by:

$$P_{noise} = \sigma^2 \implies \sigma = \sqrt{P_{noise}} \quad (\text{C.5})$$

This calculated σ is then used as the standard deviation for generating the Gaussian noise samples.

Appendix D. Autoencoder Implementation

A standard autoencoder neural network is implemented in this work to compress input data and subsequently reconstruct it for the purpose of anomaly detection. The core concept involves learning a lower-dimensional representation that captures the essential features of the input and measuring the quality of that representation in the networks ability to reconstruct the original vector. This architecture comprises two principal components: the encoder and the decoder.

The encoder’s function is to reduce the dimensionality of the input. This is done by using a sequential network consisting of two linear layers, each with a ReLU activation applied after the first linear transformation. The output z , set to 8 dimensions, represents the compressed version of x .

The decoder reverses this process, attempting to reconstruct the original input from the compressed representation. It also consists of two linear layers, with a ReLU activation following the first, and a sigmoid activation at the output. The output \hat{x} is the reconstructed input.

For training, the Mean Squared Error (MSE) loss function is used, which calculates the average squared difference between the input x and the reconstructed \hat{x} :

$$\text{Loss} = \text{MSE}(x, \hat{x}) = \frac{1}{n} \sum_{i=1}^n (x_i - \hat{x}_i)^2, \quad (\text{D.1})$$

where n is the dimension of the input vector. For our implementation we use an Adam optimizer and a learning rate of 0.001.

We use PyTorch for our autoencoder implementation. The data is processed in batches of 8, and the model is trained for 10 epochs. The autoencoder is applied using a sliding window approach: training on a baseline, followed by evaluation on subsequent data. This methodology allows for the detection of anomalies by observing increases in the reconstruction error when the evaluation data is not of the same form as the training baseline. This process enables the identification of anomalies through changes in the reconstruction loss.